EVALUATION OF HIGH VOLTAGE REFLECTIONS AND THEIR INFLUENCE ON VOLTAGE STRESS ON MOTOR INSULATION SYSTEMS

Thomas Hammarstroem[1*]

[1]Chalmers University of Technology, Sweden

[*]Email: thomas.hammarstrom@chalmers.se

The presence of PWM waveforms in electric driven vehicles and within the electric power engineering industry overall is generally increasing today. Shorter rise time increases the probability for voltage wave reflections within the motor windings due to impedance mismatches which is known to increase the voltage stress exposure as it introduces superimposed voltage oscillations. This work elaborates these kinds of stresses on random wound motor insulation material when applying square shaped voltages. The impact on the resulting partial discharge (PD) distribution due to this kind of excess stimuli is investigated and a specialized test set-up utilized to generate a controllable waveform for these tests, which enables a high level of flexibility. It is observed that the charge polarity and magnitude of the initial overshoot pulses influence the consequent ones strongly, suggesting a strong interaction of space charge activity. Due to this, the number of oscillations with sufficient magnitudes and width will influence the total PD exposure and the inception voltage (PDIV). Also, observations suggest that a sufficiently thin overshoot may have less influence on the PDIV level, which is significant when performing insulation coordination of motor winding material.

Keywords: PARTIAL DISCHARGES, DIAGNOSTICS, OVERSHOOTS, PWM & MOTOR WINDING

1. Introduction

The process of increased electrification has resulted in a rapid development of new, more efficient inverter drives solutions. In electrical motors applications, the level of switching loss has been reduced significantly as shorter rise times have been introduced. The drawback is an increased electrical stress on the insulation systems involved particularly when applying PWM waveforms with ultra short rise times [1, 2]. It is therefore of vital importance to enhance the insulation system performance in electrical motors appropriately to meet these challenges. One approach is to limit the presence of partial discharges (PDs), which are considered detrimental to the insulation material [1 -3] as well as a source of EMI emissions which can disturb vehicle electronics and communications.

Measurements of Partial Discharge (PD) activity are commonly used for diagnosing insulation systems status and the methodology is well established for sinusoidal waveforms at 50/60 Hz [4] or tested with closely to ideal square shaped voltages with unipolar polarity [3].

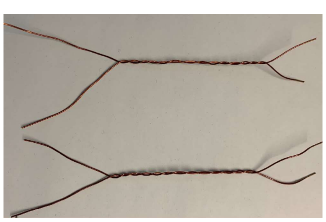

Fig. 1. The type of 1.2 mm test objects utilized in this work.

This work discusses the importance of conducting a proper evaluation of insulation status by applying electrical stress in motor windings for waveshapes which more closely resemble the actual waveshapes appearing in electric power-driven applications. The short rise time used results in overshoots due to impedance discontinuities within the electrical motors. This results in increased voltage levels and the probability for PD exposure increase.

It is difficult to investigate this phenomenon without suitable equipment which can be accurately controlled. The voltage waveform in this work is very flexible and has clearly defined flanks adjustable width of each pulse. This work will elaborate further on the relation between voltage waveforms and PD exposure

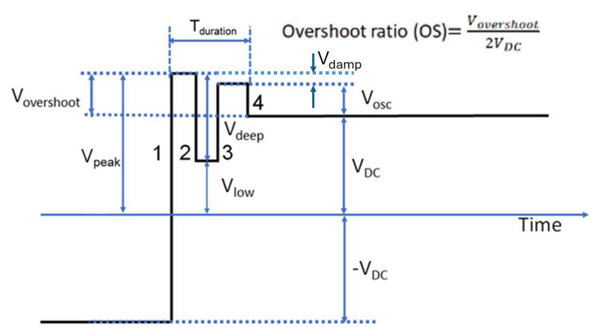

Fig. 2. The waveshape employed in this work. The sizes of flanks 1-4 are controllable as well as their duration.

as initiated in [6 -7]. Performing this adequately will most likely be a vital part in future design of electrical vehicles where the battery voltage level is increased to 800 V and beyond [5].

The aim of this work is to further explore the resulting PD characteristics and its dependence of voltage waveform dependent on overshoot levels and pulse width for a more complex waveform than [6] when exposed to a 1.2 mm grade 2 copper wire of the same type as used in randomly wound motor applications. A further objective is to explore the relation between PD appearance and the pulse width of the overshoot, as the usage of shorter rise times, increased carrier frequency as well as the utilized cable lengths are all parameters that most likely will influence the frequency and magnitude of the overshoot oscillations exposed to the insulation system.

2. Experimental Approach and Conditions

The work both presents the suitable set-up for the generation of the voltage waveform as well as the diagnostic tools utilized to identify PDs within the captured traces. The tests were performed at room temp (21 deg℃) and a relative humidity of 30%.

2.1 The controllable waveshape

To generate the complex voltage waveshape with adjustable properties, a novel test set-up is utilized which allows a flexible usage of over peak magnitudes as well as different DC voltage levels. The aim is to generate a waveshape design to resemble overshoots on a two level PWM inverter as described in fig. 2.

To implement such a waveform, a set-up is needed in which the output can be adjusted for: the risetime, overshot ratio, and DC voltage level each controllable independently. The circuit set-up designed to produce such waveforms is illustrated in fig. 3 and

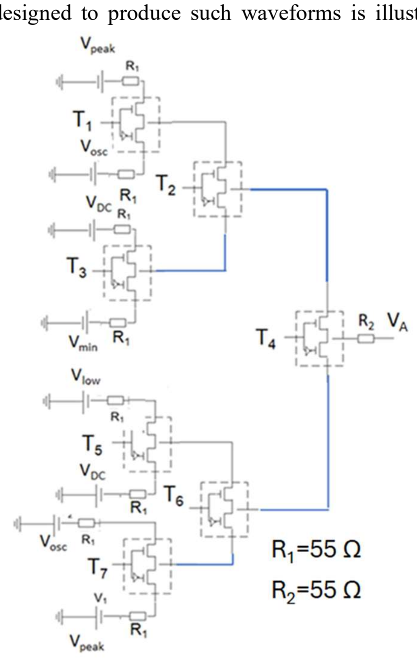

Fig.3. The arrangement of the bipolar square shaped waveform with the possibility to generate a simulated voltage overshot at both polarities. Test object is connected in point V_A. The resistor values (R_1 & R_2) used during these tests.

Table 1. Controlling scheme of the two-level inverter presented in fig. 3, which creates a simulated voltage overshot. '1' represent high input to voltage switch and '0' low input; '-' indicate no Influence on the output.

V_{out}	T_1	T_2	T_3	T_4	T_5	T_6	T_7
$V_{overshoot}$	1	1	-	1	-	-	-
$V_{DC}+V_{osc}$	0	1	-	1	-	-	-
V_{DC}	-	0	1	1	-	-	-
V_{low}	-	0	0	1	-	-	-
$-V_{low}$	-	-	-	0	1	1	-
$-V_{DC}$	-	-	-	0	0	1	-
$-V_{DC}-V_{osc}$	-	-	-	0	-	0	1
$-V_{overshoot}$	-	-	-	0	-	0	0

utilizes seven identical Behlke high voltage switches (HTS 151-03-GSM). The principle is to use each switch when selecting a specific voltage level. This implies that the voltage magnitudes can be adjusted individually, as well as time of exposure and slew rate. The various alternatives are obtained by utilizing the schedule described in tab.1. The control signals to the switches are generated by seven Agilent 33220 waveform generators. One waveform generator acts as the master trigger signal, which controls all the others, as slaves to generate the desired two-level waveform, whereas eight voltage sources present the desired voltage magnitudes. To generate the waveform utilized, a common risetime is used for all the flanks controlled by the R_1 value. In addition, equal impedance level in each path should be ensured by using the same type of cables and keeping them short as possible. This to ensure as equal risetime on all the flanks as possible.

2.2 Identification of PD activity

The most common method to identify PDs in motor windings is to filter out the remnant from the applied voltage following the standard procedure described in [7]. As the modern inverter waveform has considerably higher frequency content than sinusoidal 50 Hz [5], other measurement approaches are required to detect the presence of PDs. Examples of such are UHF or VHF

R_m (Ω)	C_u (pF))	C_b (pF)	R_u (kΩ)	R_b (kΩ)	l_m(m)
20	15	5	25	0.2	6

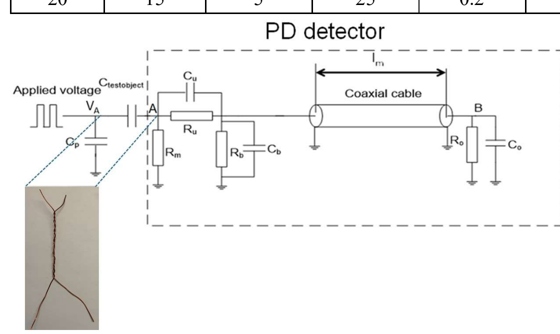

Fig. 4. High pass filter circuit for detecting PDs at steep PWM waveforms. The data collection is done by means of a high frequency oscilloscope connected to point 'B' with input impedance of R_0=1 MΩ and C_0=15 pF. Note the indicated position of the test object.

antennas and current transformers as exemplified in [8]. In this work a high pass filter is utilized as shown in fig. 4 to measure PDs. The set-up is illustrated in fig. 4 consisting of the high pass filter connected to the test object. A capacitor C_p of 50 pF was connected between point "A" and ground. The circuit represents a high pass filter, which in combination with a 4 m coaxial cable (marked as l_m in fig. 4), introduces high frequency resonances in the filter transfer function [9]. The combination of the filter circuit and the coaxial cable creates resonances which efficiently suppress the contribution from applied voltage, while at the same time amplifies the PD signal.

The aim is not necessarily to totally remove the contribution from the applied voltage with the filter but to reduce the remnant sufficiently to allow for signal processing methods to identify the PDs within the waveform. Here different approaches can be used such as AI or wavelet theory [10, 11]. Here is, however, the difference between the stable voltage remnant and the PDs employed. The latter appears stochastically in the trace. Thus, after each new waveform signal is collected, the non-stationary data containing PDs can be identified by removing the calculated average waveform from the latest captured trace [9]. By this procedure, important parameters, such as voltage level at which PDs start to appear (the inception voltage, PDIV), the lowest voltage magnitude where PDs can still be observed (the extinction voltage, PDEV), as well as the pulse repetitive PD pattern (PRPD) can be identified, also for complex multi-level inverter voltage waveforms [12], which makes the approach suitable for this study.

3. Measurement results

This study will focus on elaborating the electrical stress for both excess voltage levels resulting in high level of PD activity as well as for voltage levels close to PDIV level. One big advantage with this set-up is the ability to study the relation between electrical stress and waveform also covering cases which may not occur in reality, but with facilitate the general understanding of insulation performance in demanding applications. In the first part the PD activity will appear on several flanks and in the latter will focus more on the influence of pulse width and time delay on the first flank after polarity shift.

The level of voltage overshot ratio (OS) is here defined as illustrated in fig.2.

For data collection, a Tektronix DPO 7054 oscilloscope with a utilized sample rate of 2.5 GS/s and bandwidth of 500 MHz is employed. A LeCroy PPE probe employed for measuring the high voltage waveform.

3.1 Study of PD activity at excess voltage levels

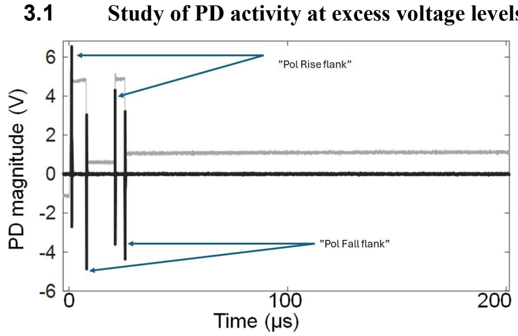

Fig. 5. A waveform will low V_{DC} voltage (0.75 kV_p) and exaggerated overshoot pulses to illustrate even distribution of PD activity at the flanks.

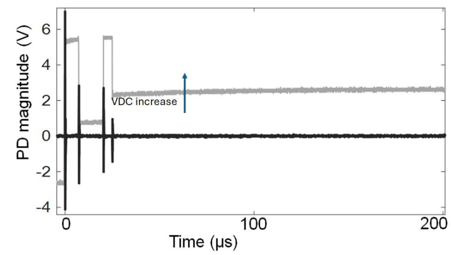

(a) The PD distribution with enlarged DC level (1.5 kV_p) , note reduced PD activity on flank four.

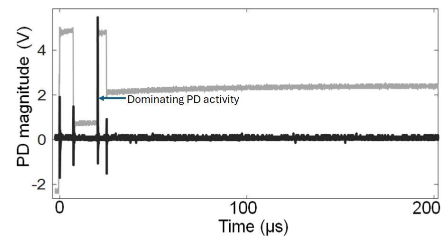

(b) Note the largest PD magnitude on flank three.

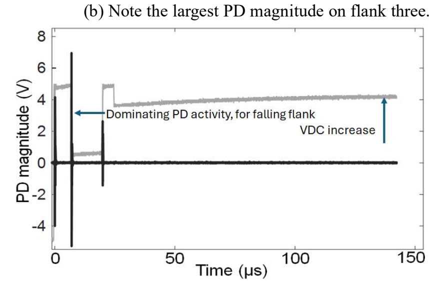

(c) Increased DC level and now PD activity on only three flanks. Note in this example the largest PD activity is on flank two.

Fig. 6. Some different traces of PD detected while increasing the V_{DC} levels.

The PD pattern appears symmetrically at both polarity shifts, therefore the shift between negative and positive is mostly presented when studying the relation between voltage flanks and PD activity.

Initially, a 0.75 kV_p DC voltage was applied with an employed additional overshoot peak of 2.25 kV_p, as illustrated in fig. 5. The aim is first to introduce PD activity on all four flanks and from there see relation between their appearance when altering the waveform.

When employing a high pass filter to resolve the PD activity, the oscillation in the measured signal often makes it difficult to reveal the polarity of the PDs. One way to study PD polarity, can be to use the recreation method on the measured PD trace to study the voltage drop in point 'A' in fig. 4 [9]. However, the trace in fig. 5 clearly directly indicates a polarity change at the different flanks as indicated, thus with the added charge level counteracting excess electric field level. This also means when overshoots are present, that the resulting charge distribution will clearly influence the next PD event in a more complex way than with only PDs appearing at the polarity shifts. The polarities and the frequencies of the appearing PD distribution then resembles the utilization of a rapidly higher voltage frequency. From this, it can be speculated that overshoots with a low level of decay will cover a large part of the

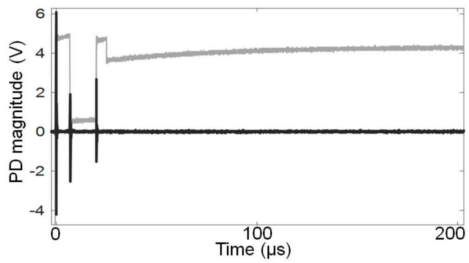

(a) With largest PD magnitude on the first often more evenly distributed on the consequent ones.

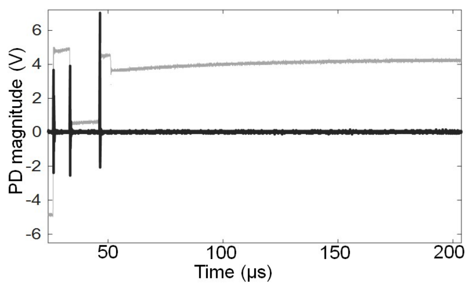

(b) Largest PDs on other flank than the first is still common, connected to minor ones at the previous flanks.

Fig. 7. Example of PD traces with consistent PD activity.

waveforms and thus result in a considerably increased level of stress and degradation.

Increasing "V_{DC}" to 1.5 kV_p in fig.6(a). results in PD activity similar as before on the first three flanks but not on the fourth, which suggests that the level of damping of the oscillations before the DC level is indeed strongly influencing the resulting PD characteristics. Generally, the PD activity on the fourth remains considerably lower in amplitude unless the "V_{DC}" level is kept close to 0 kV.

In case (b), the relation between the PD magnitude at the first two flanks is about the same and it can be noted the one at the third flank gets significantly higher although the flank size is lower than the first one.

When comparing the traces in fig. 6(a)-(c), it can be observed that the largest PDs do not always appear at the polarity shift although the magnitude of the first flank is by far the largest. It is thus observed that all three flanks can be the location of the largest PDs, see fig.7(a)(b) for further illustrations. Overall, these observations mean it is important to identify PD activity in all parts of the oscillations if the total PD amount is to be quantified. This can be a challenging task if the overvoltage waveform is large in amplitude and contains a dense oscillation.

Further this variation in magnitudes, naturally, underlines the influence of previous PD activity in the insulation system. When the summed amount of charges from previous flank is influences previous ones, clearly large magnitude PDs can still occur although the consecutive flank is lower in magnitude. Observing the PRPD pattern in fig. 8(a) reveals that the PD activity overall remains about equal on all flanks. Reducing the flanks two and three by increasing "V_{low}" results in PD activity mainly at the first flank as shown in fig.8(b), similarly as observed previously for pigtail insulation [13]. Less influence can be noted however, when comparing the peak magnitude of the PDs only.

One additional research question is how decreasing the width between the first two flanks can influence the PD distribution. Fig.8 (c) highlights that when decreasing the first pulse width to less

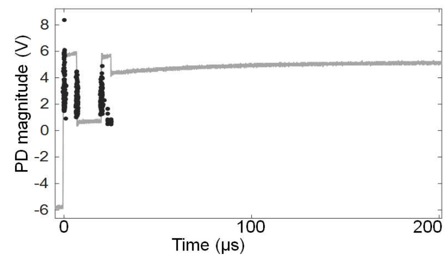

(a) PRPD pattern very simultaneously distributed

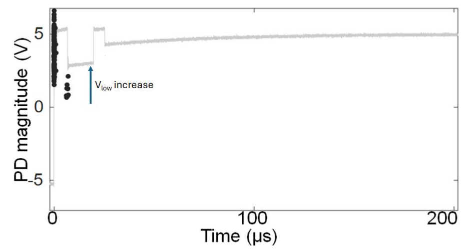

(b) Increased "V_{low}", note PD activity concentrated on one flank.

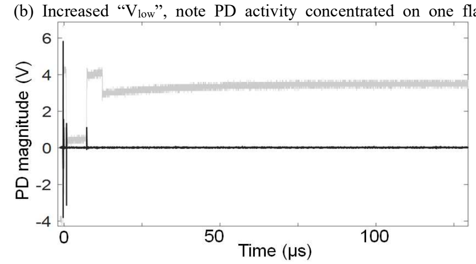

(c) A thinner first pulse is able to result in PDs at three flanks.

Fig. 8. The PRPD pattern for waveforms with both very significant oscillations (a) compared to more limited ones (b). In case (c) a 1 µs wide overshoot pulse.

than 1 µs, still PD activity can observed at three flanks. Now, to elaborate the relation between the presence of PD activity and pulse width, the waveform is modified. The DC voltage is reduced close to zero resulting to only thin pulses then, as illustrated in fig.9, occasional pulses do not result in PD activity. This observation suggest that there are cases where the conditions for PD appearance may not be fulfilled although the applied voltage level is well above PDIV, similarily as observed for paper oil insulation in [14].

The intricate task to study PD distribution is in the following section continued utilizing the original waveshape and with voltage levels that are much closer to the PDIV level.

3.2 Study of PD activity at PDIV level

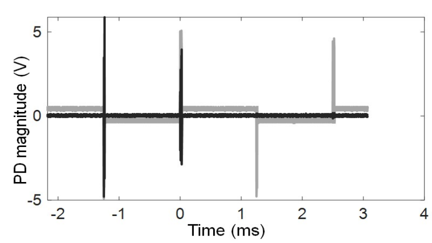

Fig. 9. A 1 µs wide overshoot pulse. Note that some pulses do not result in PDs.

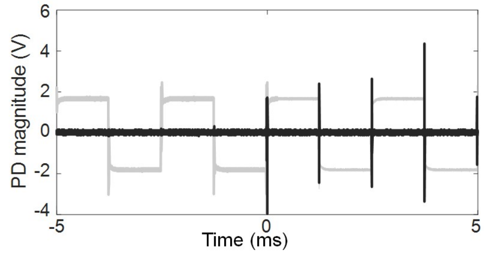

(a) Initiation of PD activity

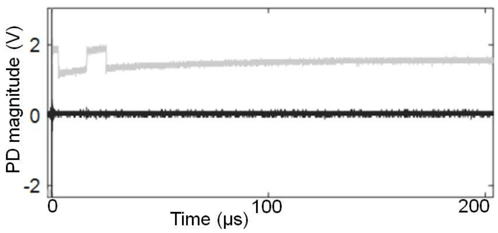

(b) Thinner first pulse with PDs still appearing at the first one.

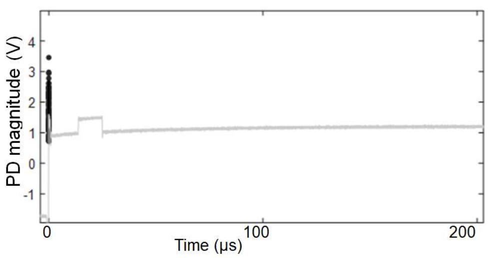

(c) The PD activity strongly connected to the rising front. Normally more distributed along the waveform close to PDIV level.

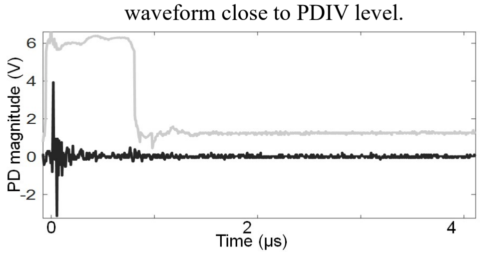

(d) At lower voltage and short rise time, less connected to the front.

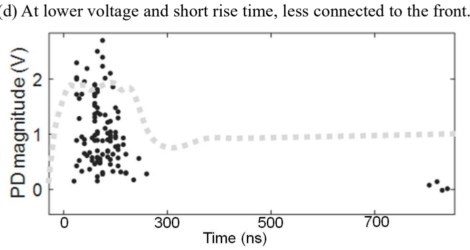

(e) PD distribution with about 300 ns pulse width versus indicated pulse shape. Note that the pulse is almost covered in PD occurrence.

Fig. 10. PD traces and PRPD pattern for PD characteristics close to PDIV level.

This section will continue to study the influence of pulse width on PD activity further. The aim is to explore the voltage distribution close to the PDIV level. The focus here is on the first overshoot peak, denoted flank '1', as it is observed that the decreased peak voltage mainly results in PD activity on the first voltage flank. The waveshape has sufficient peak magnitude to introduce PDs at the first, thin pulse followed by a significantly wider one with 150 V lover peak voltage.

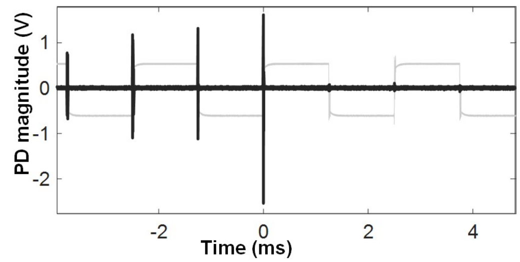

Fig. 11. Occasional loss of PD activity at certain cycles at 1.6 kV_{pp}. For wider pulses, no loss is noted.

The voltage levels for all pulses are then gradually increased until consistent PD activity can be observed, which appears on the first flank after each polarity shift as illustrated in fig10. (a)-(d). Notably very few PDs appear on other places than at the first overshoot pulse. When the pulse width is reduced to about 300 ns in fig.10(e), which is the shortest pulse employed in this text, the PD activity is still concentrated within the pulse and not on the flank. Generally, the waveforms show more flanks without PD activity also for this more complex waveform than in previous section when gradually decreasing the overshoot width, suggesting there is a limit of how thin pulses can inflict PD activity. In fig. 11 it is exemplified how the PD activity is lacking at certain flanks for the thinner pulses.

4. Discussions and conclusions

This work shows that the level of overshoot significantly influences the PD distributions in motor winding insulation systems also when the pulse width is shortened to about 1 μs. The polarity of the PDs appears to change consistently between the overshoot flanks which in principle resemble an exposure of PD activity at considerably higher frequency due to the overshoot impulses.

It was also observed that the largest magnitude PDs do not necessarily appear at the first front, rather the location of this varies as long as the flanks remain at a sufficiently high level. This was even observed for all flanks, in case flank 1 for one polarity was low then flank 2 in the following could have larger magnitude also as exemplified. One reason behind this can presumably be that less than the complete defect volume is discharged at previous PD events, leaving unchanged charge distribution. Consequently, this may result in a larger discharge at the consecutive flanks although the voltage magnitude of this step is close to PDIV level. This underlines the close relation between space charge distribution from previous discharges and new PD appearance during the overshoot oscillations. Further, this results in a more even PD magnitude distribution between the flanks as exemplified in fig.8(a).

The relation between flank size and increase in total PD resembles the observations for the motor pig tail insulation system investigated in [13].

Table 2. The average maximum PD magnitude per cycle for the case in fig.5 and fig. 8.

Case	Avg Max PD (V)
4-flank	6.15
3-flank	6.06
1-flank	5.25

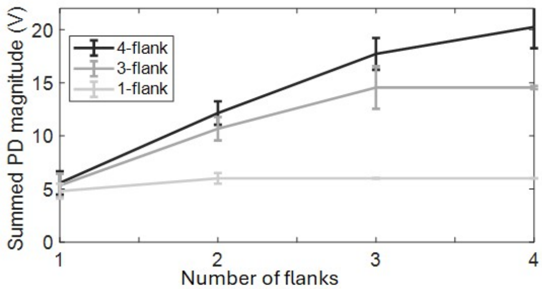

Fig. 12. The total summed PD magnitude level for various V_{DC} and V_{deep} levels as discussed in fig.5 -8.

Comparing the summed PD characteristics for the waveforms with different V_{DC} magnitudes and V_{low} levels, fig. 12 illustrates how the characteristics change dependent on the waveform selected. Sufficiently large overshoots increase the PD exposure considerably, similarly, as observed in [13]. It is further noted that the position of the largest PD magnitude varies between the flanks. When comparing the average maximum PD per cycle for the different cases, then this value increases when several sufficiently large PDs are present, as shown in tab.2. One probable reason is the increased number of large overshoot present.

It was further observed that decreasing the pulse width below 1 µs start to result in lack of PD activity at certain pulses, which suggests that further investigations should be performed both at yet thinner pulses but also at a significant reduced voltage level, where PDs start to appear. The latter case is more the focus here, as one of the most important factors of the insulation system performance is the PDIV and PDEV level.

Closer to PDIV level, the PDs are less dependent on the location of the front and their distribution, as well as when observing the lack of PDs at more polarity shifts, this suggests that for sufficiently thin overshoots pulses, the PDIV may remain at or close to the same level as even without overshoot. This presents a possible advantage with decreasing rising times and increased carrier frequency. However, to use this as a strategy to avoid PDs, the frequency would need to be very high or combined with a control strategy of the inverter at the polarity shifts to ensure thin pulses in that area. Other strategies to ensure a reduction in overshoot magnitude are presented in [15]. More work is ongoing to elucidate this further.

Thus, to conclude, it is observed in this work that sub µs overshoots can result in no PD appearing at certain flanks. But if overshoots do appear and the oscillations are long, the exposure of PDs can increase considerably and likely reduce insulation life. If sufficiently high pulses exist, then also the probability for large PDs occur for each polarity which is a probable factor for increased degradation as well. This work should be continued exploring, for example thinner pulses and at various temperatures.

References

(1) G. A. Cavallini, "Reliability of Low Voltage Inverter-fed Motors," IEEE Int. Symp. Electr. Insul. Materials (ISEIM), 2017.

(2) G. C. Montanari, F. Negri, F. Ziani, "Partial discharge and life behavior of rotating machine wire insulation under PWM waveforms: The influence of inverter characteristics", IEEE Elect. Insulation Conf., Baltimore, 2017, IEEE. doi: 10.1109/EIC.2017.8004619

(3) D. Y. Ji, P. Giangrande, W. Zhao, G. Buticchi, M. Galea and P. Zhang, "Lifetime Model for Inverter-Fed Electrical Machines Windings Including Thermal Aging and Partial Discharge Risk," in IEEE Transactions on Transportation Electrification, vol. 11, no. 1, pp. 4371-4382, Feb. 2025, doi: 10.1109/TTE.2024.3461831.

(4) IEC Publications 60270, "Partial discharge measurements", 3rd ed. 1998.

(5) W. Lee, B. -S. Lee, J. -H. Ahn, J. -Y. Kim and J. -K. Kim, "New Combined OBC and LDC System for Electric Vehicles With 800 V Battery," in IEEE Transactions on Industrial Electronics, vol. 69, no. 10, pp. 9938-9951, Oct. 2022, doi: 10.1109/TIE.2022.3148730.

(6) T. J. Hammarstroem, "Influence of Voltage Overshoot in Enamel Wire Winding Insulation Systems," 2023 IEEE Conference on Electrical Insulation and Dielectric Phenomena (CEIDP), East Rutherford, NJ, USA, 2023, pp. 1-5, doi: 10.1109/CEIDP51414.2023.10410566.

(7) IEC 60851-5 Winding wires - Test methods - Part 5: Electric properties.

(8) T. Hammarstroem, "Evaluation of different approaches to measure partial discharge characteristics within electric motor insulation," 2022 25th International Conference on Electrical Machines and Systems (ICEMS), Chiang Mai, Thailand, 2022, pp. 1-6, doi: 10.1109/ICEMS56177.2022.9983149.

(9) T. J. Å. Hammarström, "Partial discharges at fast rising voltages," Ph.D. dissertation, Dept. Mater. Manuf. Technol., High Voltage Group, Chalmers Univ. Technol., Gothenburg, Sweden, 2014.

(10) E. Balouji, T. Hammarström and T. McKelvey, "Classification of Partial Discharges Originating From Multilevel PWM Using Machine Learning," in IEEE Transactions on Dielectrics and Electrical Insulation, vol. 29, no. 1, pp. 287-294, Feb. 2022, doi: 10.1109/TDEI.2022.3148461.

(11) L. Hao et al., "Discrimination of multiple PD sources using wavelet decomposition and principal component analysis," in IEEE Transactions on Dielectrics and Electrical Insulation, vol. 18, no. 5, pp. 1702-1711, October 2011, doi: 10.1109/TDEI.2011.6032842.

(12) T. J. Å. Hammarström, "Combination of Adjustable Inverter Level and Voltage Rise Time for Electrical Stress Reduction in PWM Driven Motor Windings," in IEEE Electrical Insulation Magazine, vol. 37, no. 1, pp. 17-26, Jan.-Feb. 2021, doi: 10.1109/MEI.2021.9290459.

(13) T. Hammarström, "Overshoot level studies of PD Exposure in High Voltage Motor Isolation," in IEEE Transactions on Dielectrics and Electrical Insulation, doi: 10.1109/TDEI.2024.3428514.

(14) E. Lindell, "Partial Discharges at Repetitive Rapidly Changing Voltages",Ph.D. thesis, ISBN 9789173853125, Chalmers University of technology, Gothenburg Sweden, 2009.

(15) T. J. Hammarström and S. M. Gubanski, "Square-Shaped Waveform Pulse Control to Minimize PD Exposure Within Motor Insulation," in IEEE Transactions on Dielectrics and Electrical Insulation, vol. 30, no. 4, pp. 1850-1857, Aug. 2023, doi: 10.1109/TDEI.2023.3262615.